Available online at www.sciencedirect.com

ScienceDirect

Geochimica et Cosmochimica Acta 131 (2014) 213–226

Geochimica et Cosmochimica Acta

www.elsevier.com/locate/gca

Appraisal of TEX_{86} and TEX_{86}^{L} thermometries in subpolar and polar regions

Sze Ling Ho [a,*], Gesine Mollenhauer [a], Susanne Fietz [b,c], Alfredo Martínez-Garcia [b,d], Frank Lamy [a], Gemma Rueda [b], Konstanze Schipper [a], Marie Méheust [a], Antoni Rosell-Melé [b,e], Rüdiger Stein [a], Ralf Tiedemann [a]

[a] *Alfred Wegener Institute, Helmholtz Centre for Polar and Marine Research, P.O. Box 12 01 61, 27515 Bremerhaven, Germany*
[b] *Institut de Ciència i Tecnologia Ambientals, Universitat Autònoma de Barcelona, 08193 Bellatera, Spain*
[c] *Department of Earth Sciences, Stellenbosch University, 7600 Stellenbosch, South Africa*
[d] *Geological Institute, Swiss Federal Institute of Technology Zürich, NO G 55, Sonneggstrasse 5, CH-8092 Zürich, Switzerland*
[e] *Institució Catalana de Recerca i Estudis Avançats, Barcelona, Catalonia, Spain*

Received 25 May 2012; accepted in revised form 6 January 2014; available online 28 January 2014

Abstract

TEX_{86} (TetraEther indeX of tetraethers consisting of 86 carbon atoms) is a sea surface temperature (SST) proxy based on the distribution of archaeal isoprenoid glycerol dialkyl glycerol tetraethers (GDGTs). In this study, we appraise the applicability of TEX_{86} and TEX_{86}^{L} in subpolar and polar regions using surface sediments. We present TEX_{86} and TEX_{86}^{L} data from 160 surface sediment samples collected in the Arctic, the Southern Ocean and the North Pacific. Most of the SST estimates derived from both TEX_{86} and TEX_{86}^{L} are anomalously high in the Arctic, especially in the vicinity of Siberian river mouths and the sea ice margin, plausibly due to additional archaeal contributions linked to terrigenous input. We found unusual GDGT distributions at five sites in the North Pacific. High GDGT-0/crenarchaeol and GDGT-2/crenarchaeol ratios at these sites suggest a substantial contribution of methanogenic and/or methanotrophic archaea to the sedimentary GDGT pool here. Apart from these anomalous findings, TEX_{86} and TEX_{86}^{L} values in the surface sediments from the Southern Ocean and the North Pacific do usually vary with overlaying SSTs. In these regions, the sedimentary TEX_{86}-SST relationship is similar to the global calibration, and the derived temperature estimates agree well with overlaying annual mean SSTs at the sites. However, there is a systematic offset between the regional TEX_{86}^{L}-SST relationships and the global calibration. At these sites, temperature estimates based on the global TEX_{86}^{L} calibration are closer to summer SSTs than annual mean SSTs. This finding suggests that in these subpolar settings a regional TEX_{86}^{L} calibration may be a more suitable equation for temperature reconstruction than the global calibration.

1. INTRODUCTION

TEX_{86} (TetraEther indeX of tetraethers consisting of 86 carbon atoms) is a sea surface temperature (SST) proxy based on the relative distribution of isoprenoid glycerol dialkyl glycerol tetraethers (GDGTs) in archaeal lipids (Schouten et al., 2002). These lipids appear to be mostly biosynthesized by Thaumarchaeota (previously known as Group I Crenarchaeota) (Brochier-Armanet et al., 2008) that are omnipresent in the global ocean. The number of cyclopentane moieties of these archaeal GDGT lipids in marine sediments shows an empirical linear relationship with the annual mean temperature of the overlaying sea surface water (Schouten et al., 2002), suggesting its

* Corresponding author. Tel.: +49 (0) 471 4831 1570; fax: +49 (0) 471 4831 1923.
E-mail address: Sze.Ling.Ho@awi.de (S.L. Ho).

http://dx.doi.org/10.1016/j.gca.2014.01.001
0016-7037/

potential as a proxy for paleoclimatic conditions. Subsequently, a mesocosm study confirmed that the relative distribution of the GDGTs in seawater indeed varies with temperature (Wuchter et al., 2004).

Since then, many more studies (for a comprehensive review see Schouten et al. (2013a)) have been carried out to scrutinize the potential of TEX_{86}, revealing that the number of rings in the GDGTs seems to be responsive to the growth temperature, and is not influenced by salinity and nutrient availability (Wuchter et al., 2004), or grazing (Huguet et al., 2006a). It was also found that the isoprenoid GDGTs are less susceptible to long distance lateral transport relative to alkenones (Mollenhauer et al., 2007; Mollenhauer et al., 2008; Shah et al., 2008), i.e. biomarkers constituting a more established seawater temperature proxy known as the $U^{K'}_{37}$ index (Brassell et al., 1986; Prahl and Wakeham, 1987). In addition, the fact that the GDGTs are found at all latitudes of the global ocean, including the polar regions that are often devoid of alkenones, suggests a potential advantage of the TEX_{86} paleothermometer in these regions.

However, there are some uncertainties and potential caveats associated with the GDGT-based proxy. In some cases GDGTs are found to be more abundant deeper in the water column than in surface waters (Sinninghe Damsté et al., 2002a; Wuchter et al., 2005; Huguet et al., 2007) and have been interpreted to reflect subsurface water temperature in some settings (Huguet et al., 2007; Lee et al., 2008; Lopes dos Santos et al., 2010; McClymont et al., 2012). Limited understanding of the processes that control the sedimentary deposition of GDGTs in marine environments makes it difficult to constrain the water depth from which the sedimentary GDGTs might have originated, thus complicating the interpretation of TEX_{86} values as SST estimates.

Initially, TEX_{86} was defined by Schouten et al. (2002) based on a global sediment core-top study ($n = 44$) as:

$$TEX_{86} = \frac{[GDGT\text{-}2] + [GDGT\text{-}3] + [Cren']}{[GDGT\text{-}1] + [GDGT\text{-}2] + [GDGT\text{-}3] + [Cren']}$$

where GDGT-1, GDGT-2, GDGT-3 denote GDGTs containing 1, 2 and 3 cyclopentane moieties respectively; and Cren′ is the crenarchaeol regioisomer. Recently, based on the comparison of the correlation of all the possible combinations of GDGTs with SST, performed on a more extensive core-top data set ($n = 396$), a modified version of TEX_{86}, known as TEX^{L}_{86} was proposed (Kim et al., 2010):

$$TEX^{L}_{86} = \log_{10}\left(\frac{[GDGT\text{-}2]}{[GDGT\text{-}1] + [GDGT\text{-}2] + [GDGT\text{-}3]}\right)$$

The main difference between these two indices is that the TEX^{L}_{86} index does not include the crenarchaeol regioisomer, which could be difficult to quantify especially in subpolar regions where its abundance is usually low. This exclusion therefore results in a better applicability of the modified equation in the subpolar realm. For study sites with SST > 15 °C, Kim et al. (2010) recommended the use of a logarithmic transformed TEX_{86}, named TEX^{H}_{86}, which is calibrated using a subset of the abovementioned global compilation excluding data from subpolar and polar regions.

TEX_{86} values can be converted to SST by means of empirical linear regressions based on global surface sediments (e.g. Schouten et al., 2002; Kim et al., 2008; Kim et al., 2010). These TEX_{86} global calibrations have been applied to infer paleoclimatic variability at various subtropical and tropical sites, such as in the Arabian Sea (Huguet et al., 2006b), the Mediterranean Sea (Castañeda et al., 2010; Huguet et al., 2011), the Gulf of Mexico (Richey et al., 2011) and the Agulhas current system (Caley et al., 2011). However, the applicability of the global sediment core-top calibrations of TEX_{86} and TEX^{L}_{86} in the subpolar and polar regions remains uncertain. Thus far there are few reported studies. In some cases, modified TEX_{86} indices and calibrations are proposed and applied, such as for Cenozoic sites in the Arctic and the Southwest Pacific (Sluijs et al., 2006; Hollis et al., 2012) and Holocene sites at the continental margin of Antarctica (Shevenell et al., 2011; Kim et al., 2012). These alternative calibrations were proposed on the basis of disagreement with other temperature proxies ($pTEX_{86}$, Hollis et al., 2012), influence of terrigenous input (TEX'_{86}, Sluijs et al., 2006), and influence of subsurface GDGTs in the sedimentary pool (depth-weighted 0–200 m calibration, Kim et al., 2012). Whilst the general applicability of these alternative calibrations remains to be tested, they do suggest the need to continue investigating the factors governing sedimentary TEX_{86} signatures. Furthermore, substantial scatter in the TEX_{86} – SST correlation especially at the low temperature end of the calibration, suggests the possibility of additional non-temperature related factors that might influence the TEX_{86} indices in these regions (Kim et al., 2010).

Therefore, this study aims at assessing the applicability of the TEX_{86} and TEX^{L}_{86} indices in low-temperature environments, especially in the Arctic, the Southern Ocean and the North Pacific. In light of the important role played by polar regions in the global climate, the emphasis of this study is on mid and high latitudes, where the annual mean surface water temperatures range from −2 to 17 °C. In addition, this study also aims at providing more TEX_{86} sediment core-top data from the Southern Ocean and the North Pacific, two regions that still suffer from a lack of geographical coverage in the present global sediment core-top data set.

2. MATERIALS AND METHODS

2.1. Sediment extraction

The 160 marine surface sediment samples (topmost cm of multicores) analyzed in this study were obtained during several scientific expeditions organized by the Alfred Wegener Institute (AWI), on various research vessels (R/Vs Polarstern, Sonne, Ivan Kireyev and Akademik Boris Petrov) in the Southern Ocean, the North Pacific, the Fram Strait and the Arctic (Fig. 1; details in Supplementary data).

All surface sediments were freeze-dried and homogenized. The extraction of GDGTs from the sediment core-tops from the Southern Ocean (ANT-XXIII/9) and the Arctic (ARK-IX/4, ARK-XI/1, Transdrift-1 and SIRRO 1997–2000) was done according to the methods reported by Müller et al. (1998). Briefly, the sediments were subjected

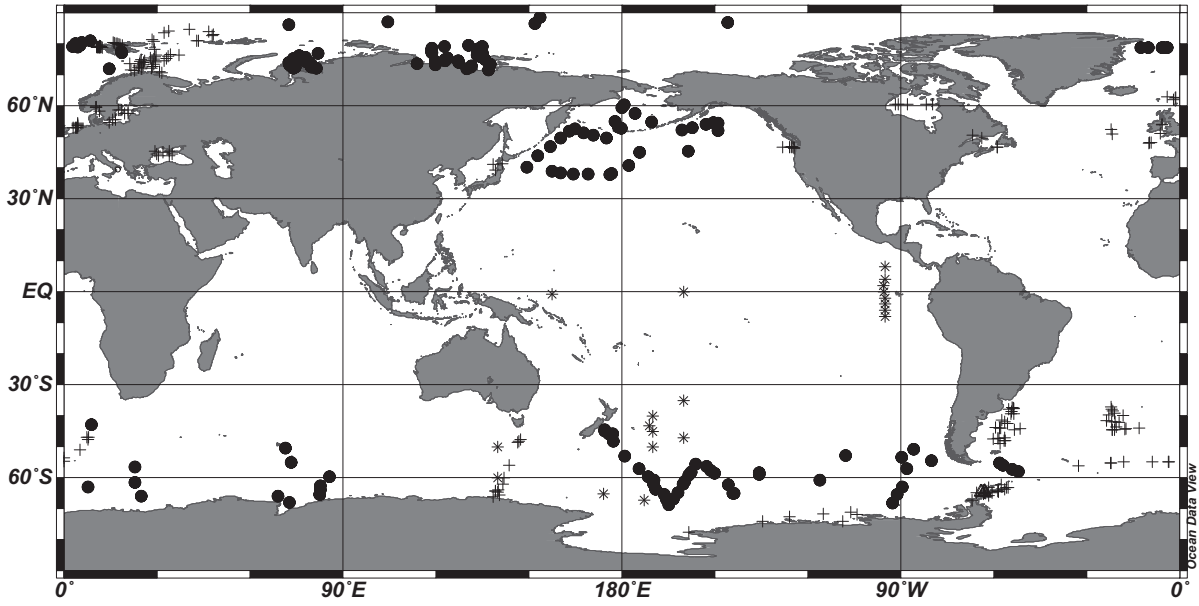

Fig. 1. Location of study sites in the global ocean. Circles denote sites in this study, while previously published data are marked by different symbols: crosses – Kim et al. (2008) and Kim et al. (2010); asterisks – Ho et al. (2011); triangles – Shevenell et al. (2011).

thrice to ultrasonication using UP200H sonic disruptor probes in successively less polar solvent mixtures (dichloromethane/methanol). For the North Pacific samples (SO202), the GDGTs were instead extracted using an accelerated solvent extractor (DIONEX ASE 350), according to the Royal Netherlands Institute for Sea Research (NIOZ) protocol (Schouten et al., 2002): heating for 5 min at 100 °C, static time of 5 min, 3 cycles and solvent mixture of dichloromethane:methanol in the ratio of 9:1, v/v. After extraction, the total lipid extracts were fractionated by open column chromatography (SiO_2 cartridges, Varian Bond-Elut) using dichloromethane/methanol.

The sediment samples from the central Arctic (ARK-XXII/2), the Fram Strait (ARK-XXI/1) and the Southern Ocean core-tops other than those from ANT-XXIII/9, were prepared using the methods described by Fietz et al. (2011). Briefly, the sediments were subjected to microwave assisted extraction by using a mixture of dichloromethane:methanol (3:1, v/v). The extracts were then injected manually into a Thermo Surveyor HPLC system equipped with a Lichrosphere Silicon dioxide column (4.6 × 250 mm, 5 μm; Teknokroma) and a stainless steel inline filter (2 μm pore size). Compound class fractionation was achieved running sequentially hexane, dichloromethane, and acetone.

2.2. Quantification of GDGTs

The GDGTs in sediment samples from expeditions ANT-XXIII/9, SO202, ARK-XI/1, ARK-IX/4, Transdrift-1 and SIRRO 1997–2001 were quantified using liquid chromatography with a method derived from Hopmans et al. (2000). The polar fractions were dissolved in hexane:isopropanol (99:1; v/v) and pre-filtered through a 4 μm diameter PTFE filter (0.45 μm pore size) to prevent clogging in the column. Filtered samples were then injected into a high performance liquid chromatography system (Agilent 1200 series HPLC system) coupled to an Agilent 6120 MSD mass spectrometer, operating with atmospheric pressure chemical ionization (APCI). The injection volume was 20 μL. A Prevail Cyano 3 μm column (Grace, 150 mm x 2.1 mm) maintained at 30 °C was used to separate the GDGTs. The injected samples were eluted with a mixture of solvents, i.e. solvent A = hexane and solvent B = 5% isopropanol in hexane. The mixture of solvents (solvents A:B in the ratio of 80:20 v/v) was eluted isocratically for 5 min, then the volume of solvent B was increased linearly to 36% in 40 min. The column was back-flushed with 100% solvent B for 8 min after each analysis to eliminate any compound remaining in the column. The spray chamber of the APCI was set in the following conditions: drying gas flow 5 l/min and temperature 350 °C, nebulizer pressure 60 psi, vaporizer gas temperature 450 °C, capillary voltage −3 kV and corona current + 4 μA. The detection of the GDGTs was achieved by Selected Ion Monitoring (SIM) of the $[M+H]^+$ ions (dwell time 67 ms) in the m/z range of 1022–1302, i.e. 1022 (branched GDGT-I), 1036 (branched GDGT-II), 1050 (branched GDGT-III), 1292 (crenarchaeol and its regioisomer), 1296 (GDGT-3), 1298 (GDGT-2), 1300 (GDGT-1) and 1302 (GDGT-0). The remaining samples (ANT-X/5, ANT-XI/2, ANT-XII/4, ANT-XX, ANT-XXVI/2, ARK-XXI/1 and ARK-XXII/2) were analyzed using the procedure described by Fietz et al. (2011).

The sample preparation was carried out at the University of Bremen, the Autonomous University of Barcelona and the Alfred Wegener Institute, while the GDGT analyses were done in the former two institutions. Results obtained from different laboratories using different analytical methods should result in comparable data because the TEX_{86} measurement is not significantly biased by extraction techniques or HPLC/APCI-MS set-ups (Schouten

et al., 2007). Subsequent interlaboratory comparison studies suggest that TEX_{86}-derived temperature estimates can differ between laboratories, in the range of 3–4 °C (15 laboratories; Schouten et al., 2009) and 1.3–3 °C (35 laboratories; Schouten et al., 2013b). However, triplicate analyses on marine sediment samples from the tropics carried out in our laboratories at the University of Bremen and the Autonomous University of Barcelona yield Branched Isoprenoid Tetraether Index (BIT) data that agree within 0.02 BIT units and TEX_{86} data that agree within 0.004 TEX_{86} units (equivalent to ~0.3 °C using the global calibration of Kim et al. (2010)), with a repeatability of better than 0.003 BIT and TEX_{86} unit in both laboratories. We note that these errors are conservative, and that for samples with lower GDGT concentrations the measurement uncertainties would be larger.

2.3. GDGT fractional abundance, TEX_{86} and BIT calculations

Fractional abundance is defined as the fraction of the abundance of an individual GDGT over the total abundance of six GDGTs (Kim et al., 2008). The values for TEX_{86} and TEX_{86}^{L} are calculated following the equations reported by Schouten et al. (2002) and Kim et al. (2010), respectively. These values are converted to SST estimates using the latest global core-top TEX_{86} and TEX_{86}^{L}-SST calibrations proposed by Kim et al. (2010). Additionally, we calculate the BIT according to Hopmans et al. (2004), which was proposed as a qualitative indicator for fluvial terrigenous GDGT input (cut-off value suggested to be 0.3 by Weijers et al. (2006)). Data with BIT values >0.3 are marked (filled with gray) in all plots to facilitate data discussion.

2.4. Environmental data

The environmental data utilized in this study, i.e. water temperature at different depths, are extracted from the World Ocean Atlas 2009 (WOA09) (Locarnini et al. (2010) data set. The WOA09 dataset is preferred over the NSIPP AVHRR Pathfinder and Erosion Global 9 km SST Climatology dataset used in Kim et al. (2010) as the latter does not contain subsurface water temperature data. However, a comparison of the NSIPP AVHRR Pathfinder SST data and the WOA09 data for all the study sites in the global calibration study of Kim et al. (2010) reveals that these two data sets are highly correlated ($r^2 = 0.99$, see Supplementary data), even at coastal sites where WOA09 has a lower geographical resolution. Exceptions to the good correlation are found at some polar sites where the Pathfinder SST data are lower, some even as low as −2.4 °C, while the lowest WOA09 SST is −1.6 °C. Considering that, in general, the freezing point of sea water in our study regions is around −1.8 °C, the lowest Pathfinder SST data (−2.4 °C) are climatically unrealistic. This suggests that the WOA09 data set is probably more appropriate for proxy calibration at low temperatures.

For comparison of our index data with seasonal mean SST, we use seasons as defined by the WOA09 (i.e. Northern/Southern hemisphere spring/autumn: April–May–June, summer/winter: July–August–September, autumn/spring: October–November–December, winter/summer: January–February–March) (Locarnini et al., 2010). Furthermore, we also investigate the empirical relationship between the GDGT indices and water temperatures weighted over 0–200 m. The calculation of depth-weighted 0–200 m water temperatures is done according to the equation described by Kim et al. (2008) and Kim et al. (2012). We wrote R scripts to retrieve the WOA09 water temperatures at various depths between surface and 200 m.

3. RESULTS AND DISCUSSION

We measured isoprenoid and branched GDGTs in 160 surface sediment samples, and calculated GDGT indices, including TEX_{86}, TEX_{86}^{L} and BIT values for these samples (Supplementary data). The distribution of isoprenoid GDGTs in our samples is similar to that in the global data set of Kim et al. (2010) except at five sites in the North Pacific and the Bering Sea (defined as Cluster 1; discussed in Section 3.1). Most samples contain an insignificant amount of terrestrially-derived GDGTs relative to the marine-derived GDGTs (as expressed by BIT values <0.3, indicated in Supplementary data), with the exception of some samples from the Arctic marginal seas with BIT values close to 1 (discussed in Section 3.2). In order to prevent biasing on the calculation of SST proxy values and the subsequent regression analyses, data associated with BIT >0.3, Cluster 1 sites, and samples with GDGT concentration below detection limit (indicated in Supplementary data) were excluded from regression analysis. For a broader geographical coverage in the appraisal of the applicability of TEX_{86} and TEX_{86}^{L} thermometries in the subpolar and polar regions, we consider also previously published data (Kim et al., 2008; Kim et al., 2010; Ho et al., 2011; Shevenell et al., 2011) from regions that are comparable in terms of SST (<17 °C) and latitudes (>37°N/S) with those presented in this study.

3.1. Fractional abundance and potential sources of GDGTs

There are substantial variations in the relationship between the fractional abundance of individual GDGTs and the WOA09 annual mean SST (Fig. 2). In a broad sense, the SST correlates negatively with the fractional abundance of GDGT-0. However, the correlations of SST with other GDGTs, i.e. GDGT-1, GDGT-2, and crenarchaeol regioisomer, do not follow a general pattern and seem to vary geographically. The distribution of GDGTs at Cluster 1 sites stands out from the rest of the data set, with elevated abundance of GDGT-0 (accounting for ~75% of the total isoprenoid GDGT pool), and to a lesser extent also GDGT-1 and -2 (Fig. 2 and Supplementary data for an example chromatogram), relative to crenarchaeol i.e. the hallmark GDGT for marine Thaumarchaeota (Sinninghe Damsté et al., 2002b). The atypical GDGT distribution in these samples suggests a contribution from an archaeal community other than the pelagic Thaumarchaeota. Soil derived-GDGTs are unlikely to be the cause, because these

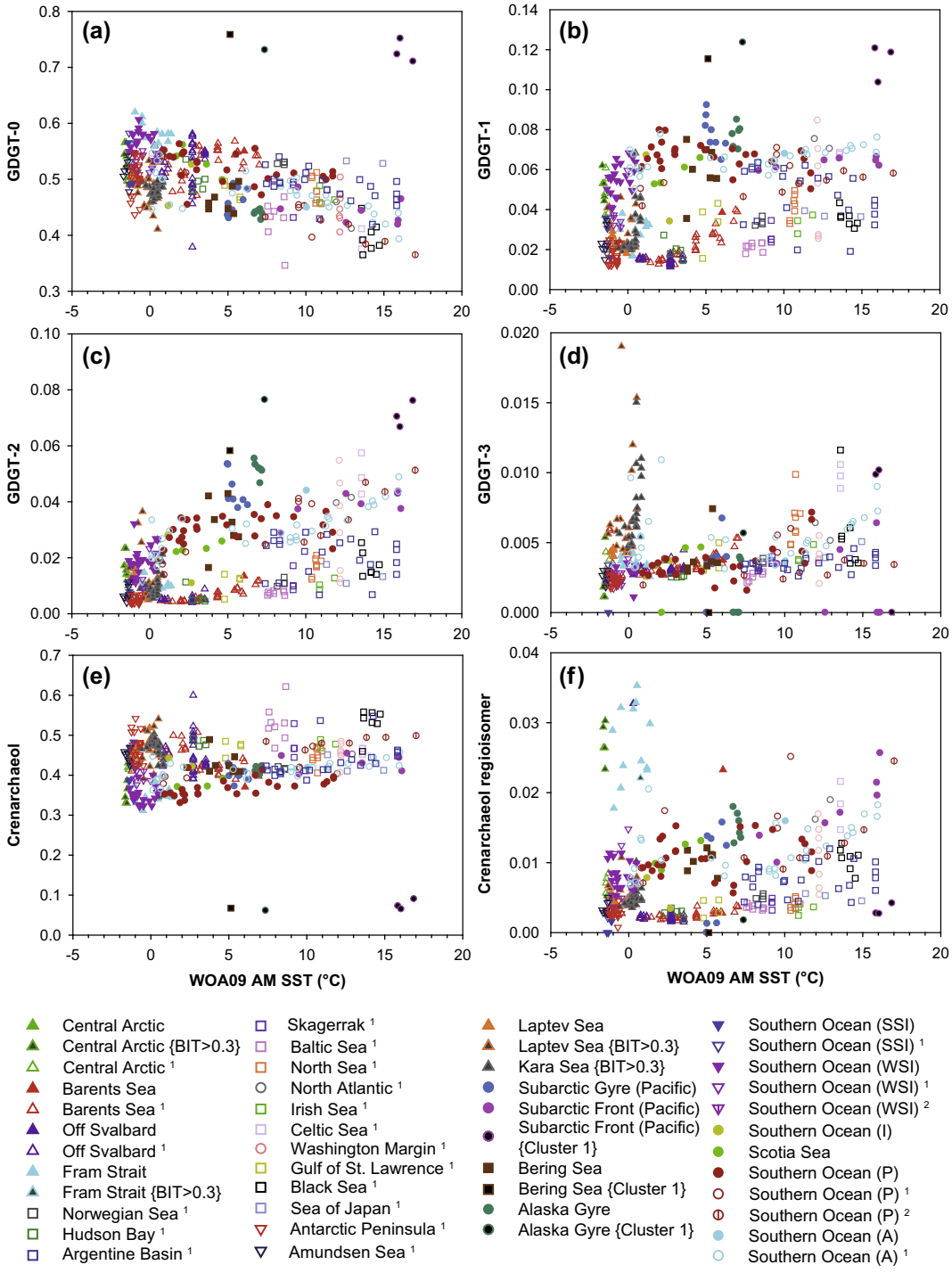

Fig. 2. Relationship between the fractional abundance of individual GDGTs and the World Ocean Atlas 2009 (WOA09) annual mean SSTs, i.e. (a) GDGT-0, (b) GDGT-1, (c) GDGT-2, (d) GDGT-3, (e) Crenarchaeol, (f) Crenarchaeol regioisomer. Oceanic regions are marked by different symbols in different colors as explained in the legends. Filled symbols indicate data from this study, open symbols indicate published data, gray-filled symbols indicate data with BIT >0.3, and black-filled symbols indicate data in Cluster 1. Abbreviations: SSI – summer sea ice; WSI – winter sea ice, I – Indian, P – Pacific; A – Atlantic. References of published data in the plots: [1] Kim et al. (2010) and [2] Ho et al. (2011).

sites are far from the coast, hence receive insignificant riverine input of terrigenous GDGTs (BIT values of these samples are below 0.05) and are not in the vicinity of the sea ice margin where ice rafted debris containing allochthonous GDGTs could be released. Among the potential contributors to these atypical GDGTs are methanotrophic and methanogenic archaea, as methane gas hydrate sites are abundant in the North Pacific (Kvenvolden and Rogers,

2005). Methane-oxidizing Euryarchaeota are known to produce GDGTs containing 0–4 cyclopentyl moieties (Pancost et al., 2001). Incidentally, our Cluster 1 samples have high Methane Index (Zhang et al., 2011) values and high GDGT-2/crenarchaeol ratio (see Table 1). Both indices are indicators for the presence of methanotrophic archaea in different settings, with values of the Methane Index > 0.5 being representative of hydrate-impacted environments while values of the GDGT-2/crenarchaeol ratio > 0.4 are associated with sulfate–methane transition zones (Weijers et al., 2011). In spite of the elevated index/ratio values in Cluster 1 samples, the relative distribution of GDGTs in these samples is different from that of methanotrophic archaea due to an overwhelming dominance of GDGT-0 (Fig. 2 and Supplementary data). This difference suggests the possibility of other archaeal sources contributing to the atypical GDGT distribution in these marine sediments, for example methanogenic Euryarchaeota, which are known to produce GDGT-0 (Koga et al., 1998). The GDGT-0/crenarchaeol ratio at these sites ranges between 8 and 12, which is remarkably high compared to the values observed in typical marine sediments (0.2–2, Schouten et al. (2002)). It has been proposed that a GDGT-0/crenarchaeol ratio > 2 is indicative of significant methanogenic archaeal input in lake sediments (Blaga et al., 2009), based on the assumption that the main contributors of GDGT-0 and crenarchaeol are the methanogenic archaea and the Thaumarchaeota, respectively. Therefore, the atypical GDGT distribution observed at Cluster 1 sites in the North Pacific and the Bering Sea might be attributable to substantial contributions from methanogens. Although there is no systematic trend in the GDGT-derived temperature residuals at Cluster 1 sites (Table 1), all Cluster 1 data are excluded from regression analysis to avoid undue bias caused by a potential GDGT contribution from archaeal groups other than the marine Thaumarchaeota. We note that with the exception of the Cluster 1 subset, the rest of our compilation satisfies the criteria of MI < 0.5, GDGT-0/Cren < 2, and GDGT-2/Cren < 0.4, suggesting that these data do reflect typical GDGT distributions in open ocean setting..

3.2. TEX_{86}- and TEX_{86}^{L}-derived SST estimates and their residuals

The residual of a SST estimate is defined here as the difference between the estimated SST using the global calibrations of Kim et al. (2010) and the WOA09 SST (i.e. residual = GDGT-derived temperature estimates – WOA09 temperature data). The standard errors of estimates for the latest global core-top calibrations for TEX_{86} and TEX_{86}^{L} (Kim et al., 2010, $n = 396$) are 5.2 °C and 4 °C, respectively (represented by gray lines in Fig. 3).

The general patterns in temperature estimate residuals differ between the TEX_{86} and TEX_{86}^{L} indices. For TEX_{86}, a separate cluster (determined visually from the plots), with positive TEX_{86} residuals ranging between ~5 and 30 °C, is apparent at the low temperature end (Fig. 3a, c, and e). This cluster consists mostly of data from the Arctic, including the central Arctic, the Laptev Sea, and the Fram Strait. In another Arctic marginal sea, i.e. the Kara Sea, the TEX_{86}-derived temperature estimates match well with the summer SSTs. A different pattern, however, is apparent in the TEX_{86}^{L} residual plots (Fig. 3b, d, and f), wherein the temperature residuals at the Arctic sites in the Fram Strait and the Laptev Sea sites are well within the estimation error. Diverging patterns in TEX_{86} residuals and TEX_{86}^{L} residuals also exist in the Southern Ocean (the Pacific sector and the winter sea ice edge) and the North Pacific (Alaska Gyre, Subarctic Front [Pacific], Subarctic Gyre [Pacific] and the Bering Sea), where most TEX_{86}-derived temperature residuals are within the estimation error of the global calibration (Fig. 3a, c, and e) while many of the TEX_{86}^{L} residuals are above the estimation error (Fig. 3b, d and f).

Remarkably, TEX_{86} derived SST estimates for numerous Arctic sites are ~30 °C higher than the summer SST at the sites (Figs. 3 and 4). Some of the warm-biased SST estimates near the coast, e.g. off Siberia, are probably the consequence of an overwhelming terrigenous overprint due to a significant input of terrestrially-derived GDGTs via Siberian river runoff from the Lena, Ob and Yenisei Rivers. As suggested by the BIT values (Fig. 4c), terrigenous GDGTs are abundant relative to marine GDGTs (BIT values close to 1) at coastal sites in the Laptev Sea and the Kara Sea, in agreement with BIT values >0.9 previously reported for Siberian Arctic estuarine sediments (van Dongen et al., 2008). In the Kara Sea and the Laptev Sea, the BIT values decrease with distance from the coast, which could be due to either a seaward increase in crenarchaeol abundance or a seaward decrease in branched GDGT abundance. The latter is a more likely reason for BIT changes in the region, judging from previous studies on terrigenous organic carbon input in the Arctic marginal seas based on *n*-alkanes. For example, Fahl and Stein (1997) found a seaward decreasing trend in the concentrations of long-chain *n*-alkanes and long-chain wax esters (both indicators of terrigenous input) in the Laptev Sea. Fernandes and Sicre (2000) also reported that the abundances of terrigenous *n*-alkanes decrease with distance from the Ob and Yenisei river mouth in the Kara Sea. These findings support our interpretation that the BIT values at our sites are mostly driven by the changes in branched GDGT abundance, hence they trace the terrigenous input from the Arctic rivers. Whilst its usefulness in quantifying terrigenous organic carbon in the Chukchi Sea has been questioned (Belicka and Harvey, 2009), it appears that the BIT is a reliable qualitative indicator for riverine input in the Laptev and the Kara Seas.

Some of the anomalously high TEX_{86} and TEX_{86}^{L} SST estimates are associated with high fractional abundance of GDGT-3 (Fig. 2), in agreement with previous work on the Arctic during the PETM, in which the authors have also found anomalously high abundance of GDGT-3 (Sluijs et al., 2006) that in turn resulted in high TEX_{86} values. The authors interpreted the deviant GDGT-3 as terrestrially originated, and discarded GDGT-3 from the TEX_{86} calculation. Nevertheless, at our study sites in the Laptev Sea and the Kara Sea, the overestimations of TEX_{86} and TEX_{86}^{L} derived temperatures are not solely related to the distance from the coast or the BIT values (hence the impact of riverine terrigenous GDGTs). In the Laptev Sea, the

Table 1
GDGT-based indices and GDGT-derived temperature residuals at Cluster 1 study sites with anomalous GDGT distribution.

Site	BIT index[a]	Methane index[b]	Ratio of GDGT-2/Crenarchaeol[c]	Ratio of GDGT-0/Crenarchaeol[d]	TEX_{86} residual[e] (°C)	TEX_{86}^{L} residual[e] (°C)
SO202/36–6	0.02	0.72	0.86	11.26	−9.24	0.30
SO202/37–1	0.02	0.77	1.25	11.94	−10.57	2.49
SO202/42–3	0.05	0.73	0.97	9.94	−7.25	1.67
SO202/11–1	0.00	0.67	0.84	7.86	−4.39	9.75
SO202/29–5	0.03	0.73	1.03	11.57	−1.01	10.52

[a] Branched Isoprenoid Tetraether (BIT) index as proposed by Hopmans et al. (2004).
[b] As proposed by Zhang et al. (2011).
[c] As proposed by Weijers et al. (2011).
[d] As proposed by Blaga et al. (2009).
[e] Residual is defined as the difference between temperature estimated using the global calibrations proposed by Kim et al. (2010) and WOA09 annual mean SST.

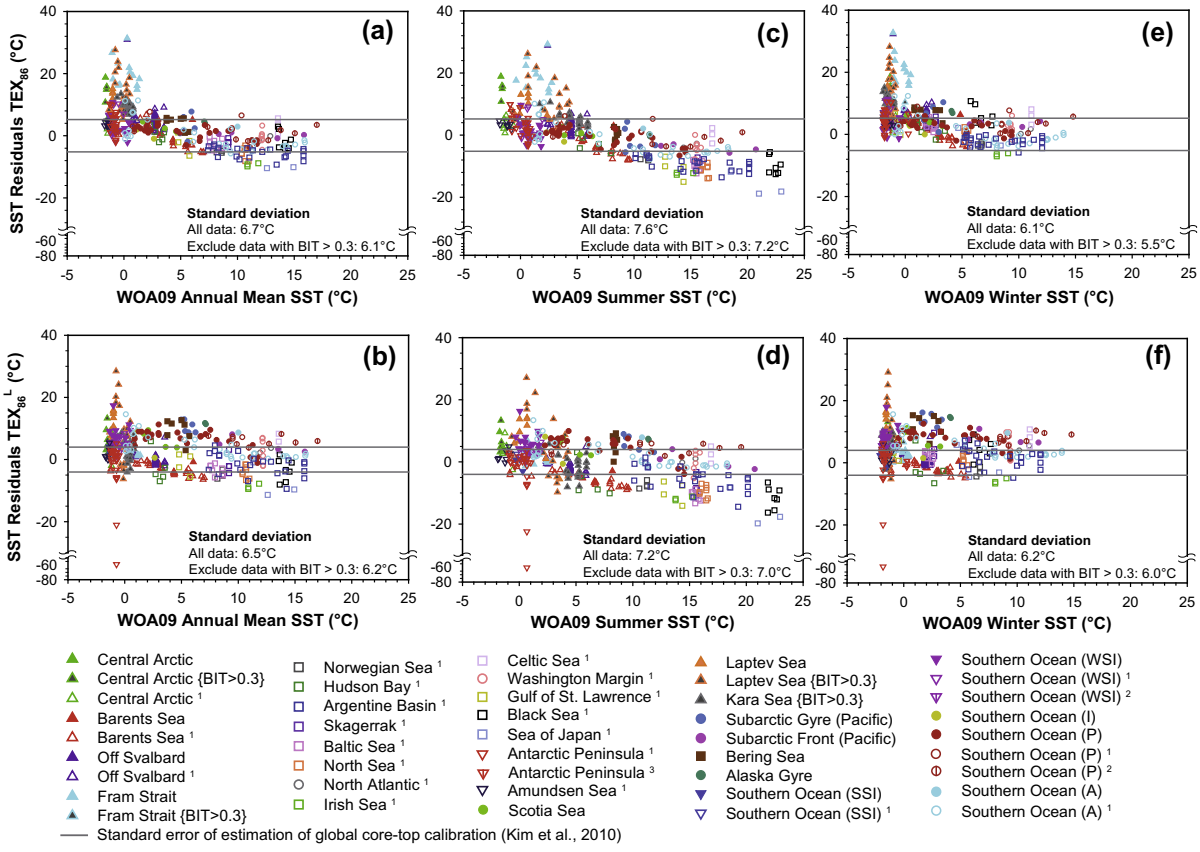

Fig. 3. The residuals of temperature estimates derived from the latest global core-top calibrations for TEX_{86} and TEX_{86}^{L} (Kim et al., 2010). SST residuals are defined as the subtraction of World Ocean Atlas 2009 (WOA09) annual mean/summer/winter SST from the estimated SST. The gray lines represent the standard error of estimates for the calibrations. Symbols and abbreviations are as in Fig. 2. References of published data in the plots: [1]Kim et al. (2010), [2]Ho et al. (2011) and [3]Shevenell et al. (2011).

extent of the overestimation at the sea ice margin and at sea ice covered sites north of the summer sea ice extent is comparable to that at the river mouth. In the Kara Sea, there is a seaward increase in the magnitude of the SST overestimation peaking in the vicinity of the sea ice margin (Fig. 4a and b), in contrast to the seaward decrease in BIT values (Fig. 4c). The mismatch between the spatial pattern of the BIT values and the warm bias in our sediment core-top TEX_{86} and TEX_{86}^{L} inferred estimates in these Arctic marginal seas suggests that terrigenous GDGTs supplied by riverine transport are unlikely the cause for the warm bias in the vicinity of the sea ice margin. Instead, the warm bias could be caused by the transport of allochthonous GDGTs via the release of ice rafted debris.

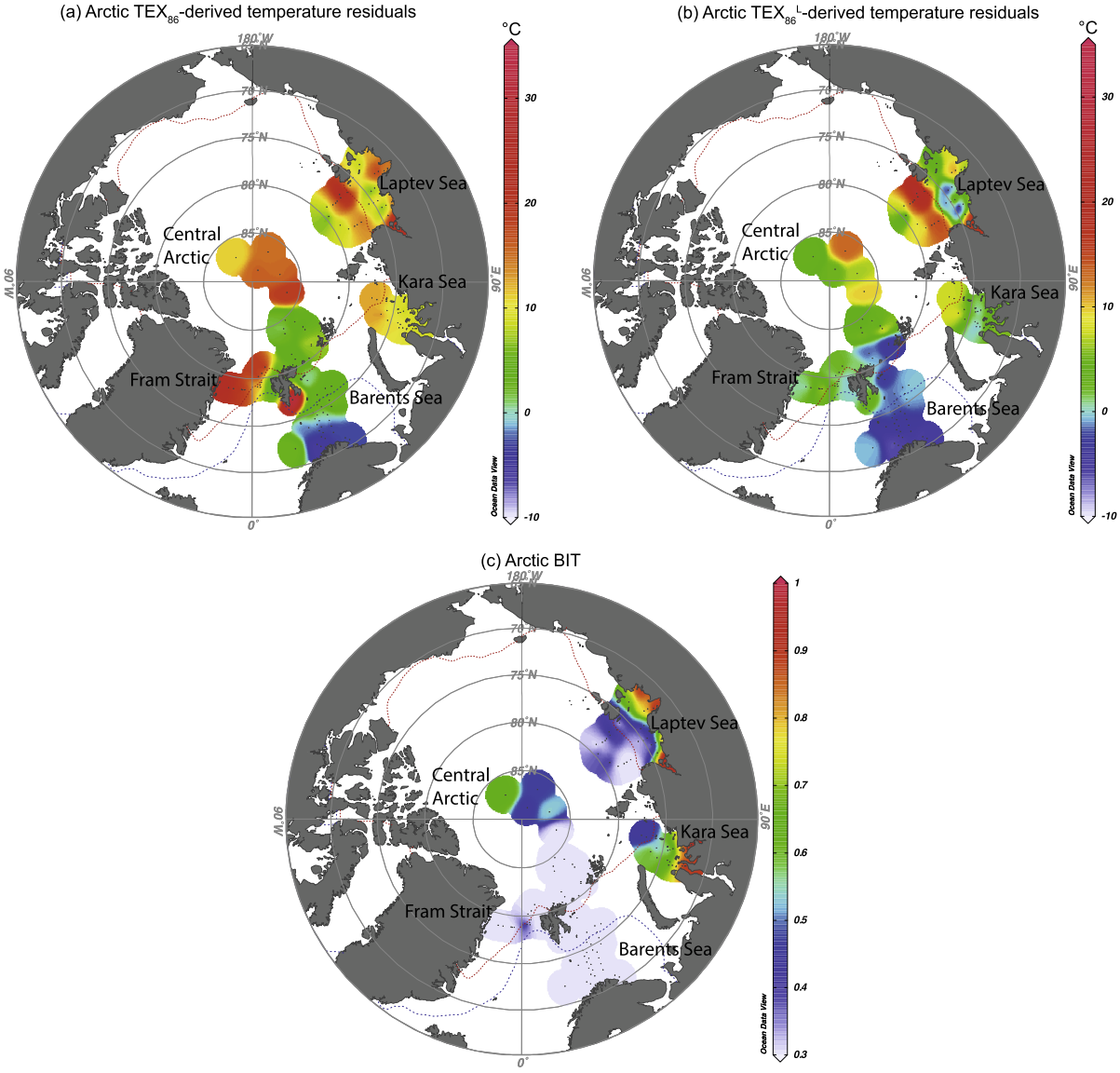

Fig. 4. Close-up of the BIT values and the residuals of (a) TEX_{86} and (b) TEX_{86}^{L} derived SST estimates relative to World Ocean Atlas 2009 (WOA09) summer SST in the Arctic. The blue and red dotted lines denote the maximum and minimum monthly sea ice extent respectively, incorporated in the Ocean Data View software (ODV; Schlitzer, 2011), and based on data from Walsh (1978) and Zwally et al. (1983). Black dots illustrate the study sites, and color bars illustrate the residuals and the BIT values.

3.3. Correlations of TEX_{86} and TEX_{86}^{L} values to water temperatures

We examine the correlation of TEX_{86} and TEX_{86}^{L} values against annual mean and seasonal SST (Figs. 5 and 6, see Supplementary data for individual cross-plot for each region). To avoid bias, Cluster 1 data (discussed in Section 3.1) are excluded from the regressions. We compare regressions through the entire data set and a reduced data set that excludes data from sites with BIT values > 0.3 (Table 2). The comparison shows that removing data points associated with BIT > 0.3 and BIT > 0.2 (not shown) result in improvement of the correlations (based on r^2 values).

Overall, compared to its counterpart TEX_{86}, the TEX_{86}^{L} displays improved correlation with the SST (Fig. 5 and Table 2). There is considerable scatter in the TEX_{86} data, especially those from the Laptev Sea, the Fram Strait and the central Arctic, which form a visually separate cluster due to their relatively high TEX_{86} values at low SSTs (discussed in Section 3.2). The most pronounced scatter in the TEX_{86}^{L}data set is attributable mainly to five data points from the Laptev Sea and two anomalous data points from the Antarctic Peninsula (data from Shevenell et al. (2011)). Both TEX_{86} and TEX_{86}^{L} values in the Southern Ocean and the North Pacific vary positively with SSTs. The regional TEX_{86}–SST relationships here follow the global pattern (Fig. 5a), especially in the Pacific sector of the Southern

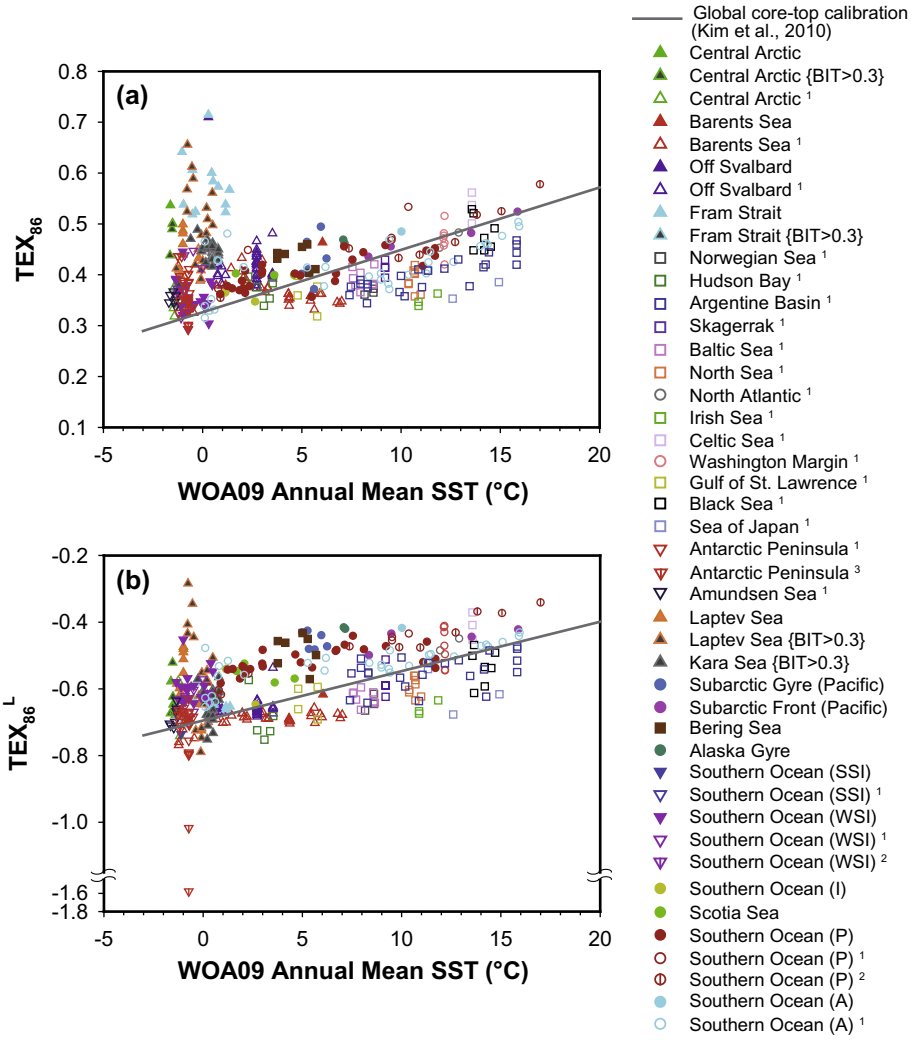

Fig. 5. Correlation plots of (a) TEX_{86} and (b) TEX_{86}^{L} values with annual mean sea surface temperature derived from World Ocean Atlas 2009 (WOA09). Gray lines illustrate the latest global core-top calibrations (Kim et al., 2010). Symbols and abbreviations are as in Fig. 2, while references are as in Fig. 3.

Ocean and the Subarctic Front zone of the North Pacific. However, there is a systematic offset between the TEX_{86}^{L}–SST relationships in these regions and that of the global calibration (Fig. 5b).

Since archaea are found throughout the water column (e.g. Karner et al., 2001), it is tempting to speculate that the lack of correlation of TEX_{86} and TEX_{86}^{L} with SST could be due to a substantial input of GDGTs from deeper waters, interfering with the surface water GDGT signal. The correlations of both GDGT indices with the SST (0 m) are not significantly better than those with the temperatures for depth-weighted 0–200 m (Table 2), suggesting that subsurface export from water depths of <200 m to the sediments cannot be ruled out entirely. This is in agreement with previous findings derived from studies on surface sediments (Lopes dos Santos et al., 2010; Lengger et al., 2012; McClymont et al., 2012) and suspended particulate matter in water column (Huguet et al., 2007; Lee et al., 2008). However, sediment core-top data, being an integration of the entire water column and of different seasons, are not suitable to disentangle the effect of subsurface GDGT export and cooler than annual mean seasonal temperature as reasons for cold-biased TEX_{86}-derived temperatures. Furthermore, the temperature data sets used for calibrations (0 m and 0–200 m) are highly correlated, thus the empirical relationships between these data sets and TEX_{86} indices do not allow us to pin-point the actual depth of origin of the GDGTs in our surface sediment samples.

3.4. Effect of sedimentation setting and/or seasonality in GDGT production

There is no significant difference between the correlation of TEX_{86} values with the annual mean SST (Fig. 5a, Table 2) and those with the seasonal SSTs (Fig. 6a–d, Table 2). The same is true for the TEX_{86}^{L} data set (Figs. 5b, 6e–h, Table 2), with the exception of the correlation with summer SST that is slightly poorer than those of the other seasons and the annual mean.

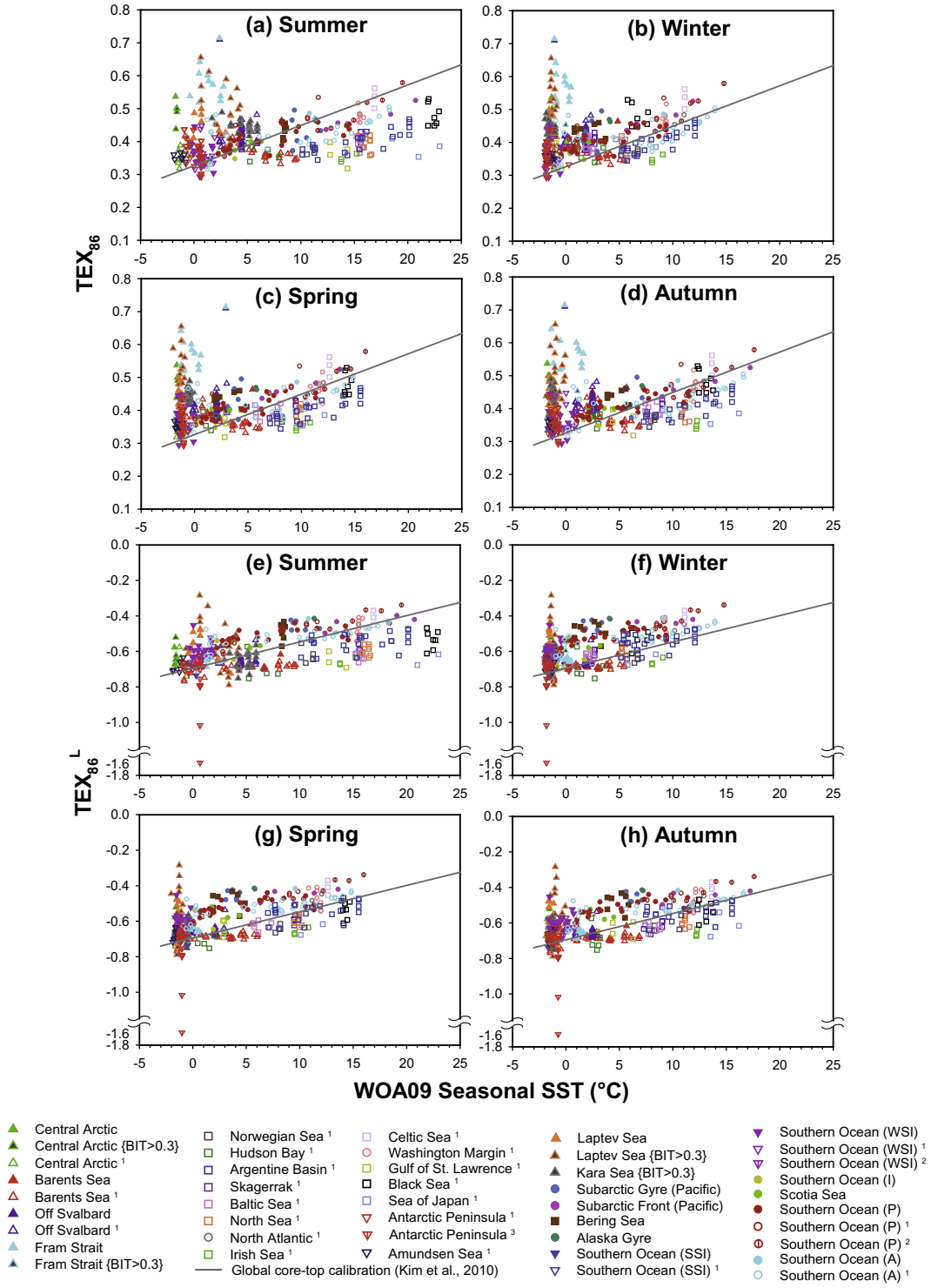

Fig. 6. Correlation plots of (a–d) TEX_{86} and (e–h) TEX_{86}^{L} values with mean seasonal sea surface temperature derived from World Ocean Atlas 2009 (WOA09). Gray lines illustrate the latest global core-top calibrations (Kim et al., 2010). Symbols and abbreviations are as in Fig. 2, while references are as in Fig. 3.

A closer inspection of the scatter plots of TEX_{86} and TEX_{86}^{L} vs. annual mean SST (Fig. 5) reveals two groups, situated above and below the global calibration of Kim et al. (2010) respectively. To some extent, the data in the group above the global calibration are from a deep, open ocean setting (e.g. Alaska Gyre, Bering Sea, Southern Ocean Pacific sector, Subarctic Gyre), while the group below the global calibration consists mostly of data from the marginal seas and/or continental shelves (e.g. Baltic Sea, Irish Sea, Black Sea, North Sea). A corresponding trend is evident

Table 2
Coefficient of determination (r^2) of linear regressions run through various TEX_{86} and TEX_{86}^L data sets. The P-values of all the regressions are < 0.0005, thus are highly significant within the confidence level of 95%.

WOA09 temperature data	Subpolar data set excluding Cluster 1 data ($n = 387$)		Subpolar data set excluding Cluster 1 and BIT > 0.3 data ($n = 339$)	
	TEX_{86}	TEX_{86}^L	TEX_{86}	TEX_{86}^L
0 m, annual mean	0.03	0.25	0.09	0.30
0–200 m, annual mean	0.03	0.23	0.11	0.29
0 m, summer	0.02	0.20	0.07	0.24
0 m, winter	0.03	0.27	0.10	0.32
0 m, spring	0.03	0.24	0.10	0.30
0 m, autumn	0.02	0.25	0.09	0.31

in the temperature residual plots, especially in those of TEX_{86}^L (Fig. 3 and depth-coded Supplementary data), wherein most of the warm-biased estimates occur at the open ocean sites, while the cold-biased estimates occur in the marginal seas and on the continental shelves. The contrasting (warm vs. cold) bias in the SST estimates at the abovementioned open ocean settings and marginal seas might be the reason why we do not observe substantial differences in the correlation with seasonal SSTs (Fig. 6), as the opposing biases might have canceled out the correlation to warm or cold seasons.

A combination of factors, including archaeal ecology, sedimentation regime and seasonality, might have contributed to the diverging TEX_{86}/TEX_{86}^L-SST relationships in different settings. The microbial communities are known to differ between coastal and open ocean regions, with latitude, and in regions where there is upwelling of mesopelagic waters to the surface (Giovannoni and Vergin, 2012). A transect study (Santoro et al., 2010) in the Gulf of California found gene copies of deep-water archaea in the surface waters of the coastal upwelling region, but not at the deeper oligotrophic offshore site. This suggests how upwelling events at coastal sites probably transport deep-water archaea to the surface, thereby resulting in different archaeal distributions in the surface waters between coastal and offshore sites. Alternatively, the cold-biased TEX_{86}/TEX_{86}^L-derived SST estimates in marginal seas might arise from higher archaeal cells/lipid abundances in winter, as reported for the North Sea (Wuchter et al., 2005; Wuchter et al., 2006) and the Antarctic coastal waters (Murray et al., 1998; Church et al., 2003). On the other hand, the GDGT flux to the seafloor in an open ocean setting (e.g. Southern Ocean, North Pacific) might be more tightly linked to the export of primary production, which is heavily biased towards the warmer seasons (Honjo et al., 2000; Honda et al., 2002) due to higher light availability, hence result in warm-biased SST estimates. Similar observations, albeit on a regional scale, were made previously in a seaward transect study in the Mediterranean (Leider et al., 2010), where the TEX_{86}-derived SSTs were increasingly overestimated seaward. The authors invoked seasonality in the production of planktic archaea, the nutrient conditions and particle loading in surface waters to explain their findings. These mechanisms might be in play as well in the marginal seas and the open oceans in the subpolar and polar regions, causing the scatter in the low and mid temperature range in the data set. Furthermore, some of the underestimation at the continental margins may also be attributable to lateral transport. This seems to be the case in the Argentine Basin (Supplementary data), where previous studies suggested that the observed cold-biased alkenone-derived SSTs are due to the advection of allochthonous alkenones by vigorous surface currents (Benthien and Müller, 2000; Conte et al., 2006; Mollenhauer et al., 2006; Rühlemann and Butzin, 2006).

Nevertheless, the abovementioned sedimentation setting-related biases may not apply to all the subpolar regions, especially at sites where temperature estimates inferred from TEX_{86} and TEX_{86}^L suggest different seasonalities for the production of GDGTs. For instance, TEX_{86}-SST relationships in the surface sediments of the Southern Ocean (Pacific sector) and the Subarctic Front in the North Pacific follow the global pattern (calibrated against the annual mean SST), while the TEX_{86}^L-inferred temperatures in these regions correspond better to the summer SST (Figs. 3, 5 and 6, Supplementary data). This is in spite of the fact that both indices are based on GDGTs biosynthesized by the same group of archaea and the indices are thus expected to reflect, if any, the same seasonality in the temperature estimates. Hence, the confirmation of our hypotheses awaits future work, in the form of water column studies, along with downcore reconstructions based on a multiproxy approach, which would allow a better constraint on the seasonality in TEX_{86} and TEX_{86}^L paleothermometries by using other independent water temperature proxies.

4. SUMMARY AND CONCLUSIONS

In this study we assess the applicability of the TEX_{86} thermometry in the subpolar and polar regions using sediment core-top data. In order to evaluate the quality of the calibrations, we examine both the correlation of our sediment core-top TEX_{86}/TEX_{86}^L values with modern SST, and the residuals of the temperature estimates (how well the estimates match the WOA09 SSTs). We found considerable scatter in the TEX_{86}/TEX_{86}^L-SST correlations in the temperature range between −2 and 17 °C, leading to large temperature residuals. Dissimilar spatial patterns in the TEX_{86}- and TEX_{86}^L-derived temperature residuals in this temperature range render the attribution of any seasonal-bias, subsurface GDGT input, or differences in sedimentation setting to the deviation, inconclusive. Furthermore,

substantial overestimates at many Arctic sites, probably due to terrestrial archaeal GDGT input, call for caution in interpreting TEX_{86}/TEX_{86}^{L}-derived temperature estimates in the Arctic marginal seas.

However, the scatter in the GDGT index – temperature correlations does not necessarily imply that TEX_{86}/TEX_{86}^{L} paleothermometry is not applicable at all at low temperatures. There is clearly a robust relationship between these indices with temperature in some subpolar regions, such as the Pacific sector of the Southern Ocean and the Subarctic Front in the North Pacific, suggesting that TEX_{86}/TEX_{86}^{L} paleothermometry might be a suitable tool for paleotemperature reconstruction there.

The choice of the GDGT index (TEX_{86} vs. TEX_{86}^{L}) and the type of calibration (global vs. regional) in paleoclimatic studies is likely to be regionally dependent. For instance, the surface sediment data presented here suggest that the global TEX_{86} calibration is likely to yield reasonable SST estimates in the Southern Ocean and the Pacific Subarctic Front zone. As for the TEX_{86}^{L} paleothermometry, the regional calibration might be more suitable here than the global calibration, given the deviation of TEX_{86}^{L}-SST correlation from the global pattern.

ACKNOWLEDGEMENTS

We appreciate the constructive comments from five anonymous reviewers and the associate editor Prof. J.S. Sinninghe Damsté which greatly improved this manuscript. We would like to express our gratitude to the chief scientists, scientists and crew members on board of R/V Polarstern, R/V Sonne, R/V Akademik Boris Petrov, and R/V Ivan Kireyev for samples retrieval during various expeditions. P. Masqué and P. Cámara are thanked for providing samples from the central Arctic (PS70 samples). Thanks also go to Dr. Carme Huguet for stimulating discussion that improved data interpretation and the writing of the manuscript. We thank Dr. Thomas Laepple for discussion on statistics and for his help in writing the R scripts that greatly sped up the retrieval of depth-weighted 0–200 m water temperatures in WOA09. We are grateful to Dr. Giuseppe Cortese for improving the readability of the manuscript. A SCAR Fellowship 2010/2011 is acknowledged for financially supporting the scientific stay of S.L.H. at the Universitat Autònoma de Barcelona. Helmholtz Graduate School for Polar and Marine Research (POLMAR) is acknowledged for funding S.L.H.'s PhD study at the Alfred Wegener Institute Helmholtz Centre for Polar and Marine Research (Bremerhaven).

APPENDIX A. SUPPLEMENTARY DATA

Supplementary data associated with this article can be found, in the online version, at http://dx.doi.org/10.1016/j.gca.2014.01.001.

REFERENCES

Belicka L. L. and Harvey H. R. (2009) The sequestration of terrestrial organic carbon in Arctic Ocean sediments: a comparison of methods and implications for regional carbon budgets. *Geochim. Cosmochim. Acta* **73**, 6231–6248.

Benthien A. and Müller P. J. (2000) Anomalously low alkenone temperatures caused by lateral particle and sediment transport in the Malvinas Current region, western Argentine Basin. *Deep Sea Res. Pt. I* **47**, 2369–2393.

Blaga C. I., Reichart G. J., Heiri O. and Damsté J. S. S. (2009) Tetraether membrane lipid distributions in water-column particulate matter and sediments: a study of 47 European lakes along a north-south transect. *J. Paleolimnol.* **41**, 523–540.

Brassell S. C., Eglinton G., Marlowe I. T., Pflaumann U. and Sarnthein M. (1986) Molecular stratigraphy: a new tool for climatic assessment. *Nature* **320**, 129–133.

Brochier-Armanet C., Boussau B., Gribaldo S. and Forterre P. (2008) Mesophilic crenarchaeota: proposal for a third archaeal phylum, the Thaumarchaeota. *Nat. Rev. Microbiol.* **6**, 245–252.

Caley T., Kim J.-H., Malaize B., Giraudeau J., Laepple T., Caillon N., Charlier K., Rebaubier H., Rossignol L., Castaneda I. S., Schouten S. and Sinninghe Damsté J. S. (2011) High-latitude obliquity as a dominant forcing in the Agulhas current system. *Clim. Past* **7**, 1285–1296.

Castañeda I. S., Schefuß E., Pätzold J., Sinninghe Damsté J. S., Weldeab S. and Schouten S. (2010) Millennial-scale sea surface temperature changes in the eastern Mediterranean (Nile River Delta region) over the last 27,000 years. *Paleoceanography* **25**, PA1208.

Church M. J., DeLong E. F., Ducklow H. W., Karner M. B., Preston C. M. and Karl D. M. (2003) Abundance and distribution of planktonic Archaea and Bacteria in the waters west of the Antarctic Peninsula. *Limnol. Oceanogr.* **48**, 1893–1902.

Conte M. H., Sicre M. A., Ruhlemann C., Weber J. C., Schulte S., Schulz-Bull D. and Blanz T. (2006) Global temperature calibration of the alkenone unsaturation index ($U^{K'}_{37}$) in surface waters and comparison with surface sediments. *Geochem. Geophys. Geosyst.* **7**, Q02005.

Fahl K. and Stein R. (1997) Modern organic carbon deposition in the Laptev Sea and the adjacent continental slope: surface water productivity vs. terrigenous input. *Org. Geochem.* **26**, 379–390.

Fernandes M.-B. and Sicre M.-A. (2000) The importance of terrestrial organic carbon inputs on Kara Sea shelves as revealed by n-alkanes, OC and d13C values. *Org. Geochem.* **31**, 363–374.

Fietz S., Martínez-Garcia A., Huguet C., Rueda G. and Rosell-Melé A. (2011) Constraints in the application of the Branched and Isoprenoid Tetraether index as a terrestrial input proxy. *J. Geophys. Res. Oceans* **116**, C10032.

Giovannoni S. J. and Vergin K. L. (2012) Seasonality in ocean microbial communities. *Science* **335**, 671–676.

Ho S. L., Yamamoto M., Mollenhauer G. and Minagawa M. (2011) Core top TEX_{86} values in the south and equatorial Pacific. *Org. Geochem.* **42**, 94–99.

Hollis C. J., Taylor K. W. R., Handley L., Pancost R. D., Huber M., Creech J. B., Hines B. R., Crouch E. M., Morgans H. E. G., Crampton J. S., Gibbs S., Pearson P. N. and Zachos J. C. (2012) Early Paleogene temperature history of the Southwest Pacific Ocean: Reconciling proxies and models. *Earth Planet. Sci. Lett.* **349–350**, 53–66.

Honda M. C., Imai K., Nojiri Y., Hoshi F., Sugawara T. and Kusakabe M. (2002) The biological pump in the northwestern North Pacific based on fluxes and major components of particulate matter obtained by sediment-trap experiments (1997–2000). *Deep Sea Res. Pt. II* **49**, 5595–5625.

Honjo S., Francois R., Manganini S., Dymond J. and Collier R. (2000) Particle fluxes to the interior of the Southern Ocean in the Western Pacific sector along 170 degrees W. *Deep Sea Res. Pt. II* **47**, 3521–3548.

Hopmans E. C., Schouten S., Pancost R. D., van der Meer M. T. J. and Sinninghe Damsté J. S. (2000) Analysis of intact tetraether

lipids in archaeal cell material and sediments by high performance liquid chromatography/atmospheric pressure chemical ionization mass spectrometry. *Rapid Commun. Mass Sp.* **14**, 585–589.

Hopmans E. C., Weijers J. W. H., Schefuss E., Herfort L., Sinninghe Damsté J. S. and Schouten S. (2004) A novel proxy for terrestrial organic matter in sediments based on branched and isoprenoid tetraether lipids. *Earth Planet. Sci. Lett.* **224**, 107–116.

Huguet C., Cartes J. E., Sinninghe Damsté J. S. and Schouten S. (2006a) Marine crenarchaeotal membrane lipids in decapods: Implications for the TEX_{86} paleothermometer. *Geochem. Geophys. Geosyst.* **7**, Q11010.

Huguet C., Kim J. H., Sinninghe Damsté J. S. and Schouten S. (2006b) Reconstruction of sea surface temperature variations in the Arabian Sea over the last 23 kyr using organic proxies (TEX86 and UK'37). *Paleoceanography* **21**, PA3003.

Huguet C., Schimmelmann A., Thunell R., Lourens L. J., Sinninghe Damsté J. S. and Schouten S. (2007) A study of the TEX86 paleothermometer in the water column and sediments of the Santa Barbara Basin, California. *Paleoceanography* **22**, PA3203.

Huguet C., Martrat B., Grimalt J. O., Sinninghe Damsté J. S. and Schouten S. (2011) Coherent millennial-scale patterns in UK'37 and TEXH86 temperature records during the penultimate interglacial-to-glacial cycle in the western Mediterranean. *Paleoceanography* **26**, PA2218.

Karner M. B., DeLong E. F. and Karl D. M. (2001) Archaeal dominance in the mesopelagic zone of the Pacific Ocean. *Nature* **409**, 507–510.

Kim J.-H., Schouten S., Hopmans E. C., Donner B. and Sinninghe Damsté J. S. (2008) Global sediment core-top calibration of the TEX_{86} paleothermometer in the ocean. *Geochim. Cosmochim. Acta* **72**, 1154–1173.

Kim J.-H., Crosta X., Willmott V., Renssen H., Bonnin J., Helmke P., Schouten S. and Sinninghe Damsté J. S. (2012) Holocene subsurface temperature variability in the eastern Antarctic continental margin. *Geophys. Res. Lett.* **39**, L06705.

Kim J. H., van der Meer J., Schouten S., Helmke P., Willmott V., Sangiorgi F., Koc N., Hopmans E. C. and Sinninghe Damsté J. S. (2010) New indices and calibrations derived from the distribution of crenarchaeal isoprenoid tetraether lipids: Implications for past sea surface temperature reconstructions. *Geochim. Cosmochim. Acta* **74**, 4639–4654.

Koga Y., Morii H., Akagawa-Matsushita M. and Ohga M. (1998) Correlation of Polar Lipid Composition with 16S rRNA Phylogeny in Methanogens. Further Analysis of Lipid Component Parts. *Biosci. Biotechnol. Biochem.* **62**, 230–236.

Kvenvolden K. A. and Rogers B. W. (2005) Gaia's breath—global methane exhalations. *Mar. Petrol. Geol.* **22**, 579–590.

Lee K. E., Kim J. H., Wilke I., Helmke P. and Schouten S. (2008) A study of the alkenone, TEX_{86}, and planktonic foraminifera in the Benguela Upwelling System: Implications for past sea surface temperature estimates. *Geochem. Geophys. Geosyst.* **9**, Q10019.

Leider A., Hinrichs K.-U., Mollenhauer G. and Versteegh G. J. M. (2010) Core-top calibration of the lipid-based and TEX_{86} temperature proxies on the southern Italian shelf (SW Adriatic Sea, Gulf of Taranto). *Earth Planet. Sci. Lett.* **300**, 112–124.

Lengger S. K., Hopmans E. C., Reichart G.-J., Nierop K. G. J., Sinninghe Damsté J. S. and Schouten S. (2012) Intact polar and core glycerol dibiphytanyl glycerol tetraether lipids in the Arabian Sea oxygen minimum zone. Part II: selective preservation and degradation in sediments and consequences for the TEX_{86}. *Geochim. Cosmochim. Acta* **98**, 244–258.

Locarnini R. A., Mishonov A. V., Antonov J. I., Boyer T. P., Garcia H. E., Baranova O. K., Zweng M. M. and Johnson D. R. (2010) World Ocean Atlas 2009: Volume 1: Temperature. In *NOAA Atlas NESDIS 68* (ed. S. Levitus). U.S. Government Printing Office, Washington, D.C., p. 184.

Lopes dos Santos R. A., Prange M., Castañeda I. S., Schefuß E., Mulitza S., Schulz M., Niedermeyer E. M., Sinninghe Damsté J. S. and Schouten S. (2010) Glacial–interglacial variability in Atlantic meridional overturning circulation and thermocline adjustments in the tropical North Atlantic. *Earth Planet. Sci. Lett.* **300**, 407–414.

McClymont E. L., Ganeshram R. S., Pichevin L. E., Talbot H. M., van Dongen B. E., Thunell R. C., Haywood A. M., Singarayer J. S. and Valdes P. J. (2012) Sea-surface temperature records of Termination 1 in the Gulf of California: Challenges for seasonal and interannual analogues of tropical Pacific climate change. *Paleoceanography* **27**, PA2202.

Mollenhauer G., McManus J. F., Benthien A., Müller P. J. and Eglinton T. I. (2006) Rapid lateral particle transport in the Argentine Basin: Molecular ^{14}C and $^{230}Th_{xs}$ evidence. *Deep Sea Res. Pt. I* **53**, 1224–1243.

Mollenhauer G., Inthorn M., Vogt T., Zabel M., Sinninghe Damsté J. S. and Eglinton T. I. (2007) Aging of marine organic matter during cross-shelf lateral transport in the Benguela upwelling system revealed by compound-specific radiocarbon dating. *Geochem. Geophys. Geosyst.* **8**, Q09004.

Mollenhauer G., Eglinton T. I., Hopman E. C. and Sinninghe Damsté J. S. (2008) A radiocarbon-based assessment of the preservation characteristics of crenarchaeol and alkenones from continental margin sediments. *Org. Geochem.* **39**, 1039–1045.

Müller P. J., Kirst G., Ruhland G., von Storch I. and Rosell-Melé A. (1998) Calibration of the alkenone paleotemperature index UK'37 based on core-tops from the eastern South Atlantic and the global ocean (60 N-60 S). *Geochim. Cosmochim. Acta* **62**, 1757–1772.

Murray A. E., Preston C. M., Massana R., Taylor L. T., Blakis A., Wu K. and DeLong E. F. (1998) Seasonal and spatial variability of bacterial and archaeal assemblages in the coastal waters near Anvers Island, Antarctica. *Appl. Environ. Microbiol.* **64**, 2585–2595.

Pancost R. D., Hopmans E. C. and Sinninghe Damsté J. S. (2001) Archaeal lipids in Mediterranean cold seeps: molecular proxies for anaerobic methane oxidation. *Geochim. Cosmochim. Acta* **65**, 1611–1627.

Prahl F. G. and Wakeham S. G. (1987) Calibration of unsaturation patterns in long-chain ketone compositions for palaeotemperature assessment. *Nature* **330**, 367–369.

Richey J. N., Hollander D. J., Flower B. P. and Eglinton T. I. (2011) Merging late Holocene molecular organic and foraminiferal-based geochemical records of sea surface temperature in the Gulf of Mexico. *Paleoceanography* **26**, PA1209.

Rühlemann C. and Butzin M. (2006) Alkenone temperature anomalies in the Brazil-Malvinas Confluence area caused by lateral advection of suspended particulate material. *Geochem. Geophys. Geosyst.* **7**, Q10015.

Santoro A. E., Casciotti K. L. and Francis C. A. (2010) Activity, abundance and diversity of nitrifying archaea and bacteria in the central California Current. *Environ. Microbiol.* **12**, 1989–2006.

Schlitzer, R., (2011). Ocean Data View, http://odv.awi.de.

Schouten S., Hopmans E. C., Schefuss E. and Sinninghe Damsté J. S. (2002) Distributional variations in marine crenarchaeotal membrane lipids: a new tool for reconstructing ancient sea water temperatures? *Earth Planet. Sci. Lett.* **204**, 265–274.

Schouten S., Huguet C., Hopmans E. C., Kienhuis M. V. and Sinninghe Damsté J. S. (2007) Analytical methodology for

TEX_{86} paleothermometry by high-performance liquid chromatography/atmospheric pressure chemical ionization-mass spectrometry. *Anal. Chem.* **79**, 2940–2944.

Schouten S., Hopmans E. C., van der Meer J., Mets A., Bard E., Bianchi T. S., Diefendorf A., Escala M., Freeman K. H., Furukawa Y., Huguet C., Ingalls A., Ménot-Combes G., Nederbragt A. J., Oba M., Pearson A., Pearson E. J., Rosell-Melé A., Schaeffer P., Shah S. R., Shanahan T. M., Smith R. W., Smittenberg R., Talbot H. M., Uchida M., Van Mooy B. A. S., Yamamoto M., Zhang Z. and Sinninghe Damsté J. S. (2009) An interlaboratory study of TEX_{86} and BIT analysis using high-performance liquid chromatography–mass spectrometry. *Geochem. Geophys. Geosyst.* **10**, Q03012.

Schouten S., Hopmans E. C. and Sinninghe Damsté J. S. (2013a) The organic geochemistry of glycerol dialkyl glycerol tetraether lipids: a review. *Org. Geochem.* **54**, 19–61.

Schouten S., Hopmans E. C., Rosell- Melé A., Pearson A., Adam P., Bauersachs T., Bard E., Bernasconi S. M., Bianchi T. S., Brocks J. J., Carlson L. T., Castañeda I. S., Derenne S., Dogrul Selver A., Dutta K., Eglinton T., Fosse C., Galy V., Grice K., Hinrichs K.-U., Huang Y., Huguet A., Huguet C., Hurley S., Ingalls A., Jia G., Keely B., Knappy C., Kondo M., Krishnan S., Lincoln S., Lipp J., Mangelsdorf K., Martínez-Garcia A., Ménot G., Mets A., Mollenhauer G., Ohkouchi N., Ossebaar J., Pagani M., Pancost R. D., Pearson E. J., Peterse F., Reichart G.-J., Schaeffer P., Schmitt G., Schwark L., Shah S. R., Smith R. W., Smittenberg R. H., Summons R. E., Takano Y., Talbot H. M., Taylor K. W. R., Tarozo R., Uchida M., van Dongen B. E., Van Mooy B. A. S., Warren C., Weijers J. W. H., Werne J. P., Woltering M., Xie S., Yamamoto M., Yang H., Zhang C., Zhang Y., Zhao M. and Damsté Sinninghe. (2013b) An interlaboratory study of TEX86 and BIT analysis of sediments, extracts, and standard mixtures. *Geophys. Geosyst. Geochem* **14**, 5263–5285. http://dx.doi.org/10.1002/2013GC004904.

Shah S. R., Mollenhauer G., Ohkouchi N., Eglinton T. I. and Pearson A. (2008) Origins of archaeal tetraether lipids in sediments: insights from radiocarbon analysis. *Geochim. Cosmochim. Acta* **72**, 4577–4594.

Shevenell A. E., Ingalls A. E., Domack E. W. and Kelly C. (2011) Holocene Southern Ocean surface temperature variability west of the Antarctic Peninsula. *Nature* **470**, 250–254.

Sinninghe Damsté J. S., Rijpstra W. I. C., Hopmans E. C., Prahl F. G., Wakeham S. G. and Schouten S. (2002a) Distribution of membrane lipids of planktonic Crenarchaeota in the Arabian sea. *Appl. Environ. Microb.* **68**, 2997–3002.

Sinninghe Damsté J. S., Schouten S., Hopmans E. C., van Duin A. C. T. and Geenevasen J. A. J. (2002b) Crenarchaeol: the characteristic core glycerol dibiphytanyl glycerol tetraether membrane lipid of cosmopolitan pelagic crenarchaeota. *J. Lipid Res.* **43**, 1641–1651.

Sluijs A., Schouten S., Pagani M., Woltering M., Brinkhuis H., Sinninghe Damsté J. S., Dickens G. R., Huber M., Reichart G. J., Stein R., Matthiessen J., Lourens L. J., Pedentchouk N., Backman J., Moran K. and Scientists E. (2006) Subtropical arctic ocean temperatures during the Palaeocene/Eocene thermal maximum. *Nature* **441**, 610–613.

van Dongen B. E., Semiletov I., Weijers J. W. H. and Gustafsson Ö. (2008) Contrasting lipid biomarker composition of terrestrial organic matter exported from across the Eurasian Arctic by the five great Russian Arctic rivers. *Glob. Biogeochem. Cycl.* **22**, GB1011.

Walsh, J.E., (1978). A data set on Northern Hemisphere sea ice extent, World Data Center-A for Glaciology (Snow and Ice), "Glaciological Data, Report GD-2", pp. 49–51.

Weijers J. W. H., Schouten S., Spaargaren O. C. and Sinninghe Damsté J. S. (2006) Occurrence and distribution of tetraether membrane lipids in soils: Implications for the use of the TEX_{86} proxy and the BIT index. *Org. Geochem.* **37**, 1680–1693.

Weijers J. W. H., Lim K. L. H., Aquilina A., Damsté J. S. S. and Pancost R. D. (2011) Biogeochemical controls on glycerol dialkyl glycerol tetraether lipid distributions in sediments characterized by diffusive methane flux. *Geochem. Geophys. Geosyst.* **12**.

Wuchter C., Schouten S., Coolen M. J. L. and Sinninghe Damsté J. S. (2004) Temperature-dependent variation in the distribution of tetraether membrane lipids of marine Crenarchaeota: Implications for TEX86 paleothermometry. *Paleoceanography* **19**, PA4028.

Wuchter C., Schouten S., Wakeham S. G. and Sinninghe Damsté J. S. (2005) Temporal and spatial variation in tetraether membrane lipids of marine Crenarchaeota in particulate organic matter: Implications for TEX86 paleothermometry. *Paleoceanography* **20**, PA3013.

Wuchter C., Abbas B., Coolen M. J. L., Herfort L., van Bleijswijk J., Timmers P., Strous M., Teira E., Herndl G. J., Middelburg J. J., Schouten S. and Sinninghe Damsté J. S. (2006) Archaeal nitrification in the ocean. *Proc. Natl. Acad. Sci. USA* **103**, 12317–12322.

Zhang Y. G., Zhang C. L. L., Liu X. L., Li L., Hinrichs K. U. and Noakes J. E. (2011) Methane Index: a tetraether archaeal lipid biomarker indicator for detecting the instability of marine gas hydrates. *Earth Planet. Sci. Lett.* **307**, 525–534.

Zwally H. J., Comiso J. C., Parkinson C. L., Campbell W. J., Carsey F. D. and Gloersen P. (1983) *Antarctic sea ice, 1973–1976: satellite passive-microwave observations, NASA Special Publications SP-459*. National Aeronautics and Space Administration, Washington, DC, p. 206.

Associate editor: Jaap Sinninghe Damste